Compact Zeroth-Order Resonant Antenna Based on Dual-Arm Spiral Configuration

Chun-Chih Liu, Pei-Ling Chi, *Member, IEEE*, and Yu-De Lin, *Member, IEEE*

***Abstract*—A miniaturized and zeroth-order resonant composite right/left-handed (CRLH) antenna based on dual-arm spiral structure is presented. The proposed dual-arm spiral unit cell is able to implement and tailor the CRLH lumped elements easily in a compact fashion. Particularly, the gap coupling between the spiral arms contributes to the series capacitance $C_{\rm L}$ and the metallic via-hole at the end of one arm results in the shunt inductance $L_{\rm L}$. The resonant frequency and thus the miniaturization factor can be simply engineered by the spiral parameters that determine the corresponding circuit elements. The proposed CRLH antenna is composed of two unit cells, each of which occupies only $0.066\lambda_0 \times 0.053\lambda_0$ at the operating frequency. From the experimental results, this compact antenna exhibits the dipole-like radiation patterns and has a peak gain of -0.53 dBi. The measured and simulated results are provided, and good agreement is achieved.**

***Index Terms*—Composite right/left-handed (CRLH), dual-arm spiral, miniaturization, small antenna.**

I. Introduction

WIDESPREAD use of the wireless communications in our daily life demands the development of compact and portable electronic products. As an essential element in the communication systems, small antennas are required correspondingly in order to fit themselves into the limited space. Numerous approaches to antenna miniaturization have been investigated. The easiest way is to employ the dielectric loading in which the antenna is built on a substrate of high dielectric constant. In spite of the substantial size reduction, the height of the antenna needs to be increased in order to compensate the deteriorated radiation efficiency [1], [2]. Similarly, the increased propagation constant in antenna structures by the capacitive loading saves the physical size at the expense of the degraded radiation characteristics and impedance bandwidth [3]. The use of relatively complicated line structures, such as the peano and meander lines [4], is beneficial for footprint reduction, while time-consuming parametric optimization and increased conductor loss make it less preferable.

The composite right/left-handed (CRLH) zeroth-order resonators may be a good alternative for implementing the miniature antennas. At the zeroth-order resonance (ZOR) mode, the infinite wavelength propagation is supported by the balanced CRLH transmission lines that exhibit uniform field distribution and increase the effective radiation aperture. Furthermore, at the zeroth-order resonance, the physical length of the resonator is independent of the resonant frequency, providing the potential for miniaturization. By engineering the constitutive lumped elements in the equivalent circuit model, the resonant frequency of the CRLH resonators can be simply tuned so as to fulfill the specific requirement [5]. Therefore, extensive studies on the CRLH zeroth-order antennas have been conducted. In order to artificially implement the CRLH unit cells, the mushroom structures are commonly used in the literature [6], [7] where edge coupling between the adjacent patches and the vertical via-hole contribute to the series capacitance and shunt inductance, respectively. The weak edge coupling provided, however, limits the attainable capacitance, and therefore the practicability of these simple structures in applications where large capacitance is required. To enhance the series capacitance, the metal–insulator–metal (MIM) structure is introduced at the expense of increased difficulty in the multilayer fabrication process [8]. On the other hand, when the coplanar antenna structures are considered, the shunt inductance is usually implemented using additional distributed meander line or shorting stub, which increases the footprint in the transverse direction [9], [10].

The single-arm spiral configuration is well known for inductor implementation. On the other hand, the equivalent capacitor can be realized through the dual-arm coupling, which is shown effective in capacitance enhancement [11]. In spite of their versatile potential for L or C implementations, less effort is made on the CRLH unit cells based on the spiral structures. In this letter, the dual-arm spiral configuration is used to build the CRLH unit cells for the zeroth-order antenna. By means of the dual-arm coupling and shorting via-hole at one of the spiral arms, the series capacitance and shunt inductance can be easily implemented in a compact fashion. Furthermore, size reduction can be simply accomplished by optimizing the spiral parameters to reduce the resonant frequency. Calculated and experimental results will be provided and compared to validate our proposed antenna.

II. Operating Principle and Parameter Investigation of the Proposed Antenna

The frequency behavior of the CRLH transmission line can be explained using the unit-cell equivalent circuit model as shown in Fig. 1 along with the dispersion curve under the balanced condition. In order to demonstrate the unique feature of the left-handed (LH) property, the series capacitance $C_{\rm L}$ and shunt

Manuscript received October 28, 2011; revised December 23, 2011 and February 07, 2012; accepted March 13, 2012. Date of publication March 20, 2012; date of current version April 05, 2012. This work was supported in part by the National Science Council, Taiwan, under Grant NSC 100-2218-E-009-027.

The authors are with the Department of Electrical Engineering, National Chiao Tung University, Hsinchu 300, Taiwan (e-mail: peilingchi@nctu.edu.tw).

Color versions of one or more of the figures in this letter are available online at http://ieeexplore.ieee.org.

Digital Object Identifier 10.1109/LAWP.2012.2191381

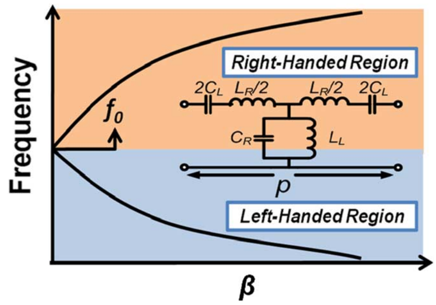

Fig. 1. Equivalent circuit model and typical dispersion curve of the balanced CRLH transmission line.

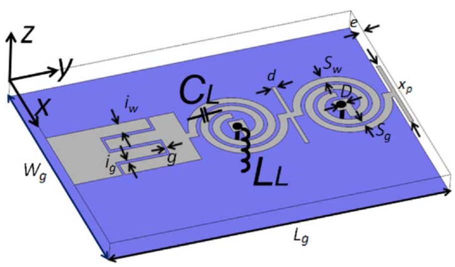

Fig. 2. Configuration of the proposed dual-arm spiral-shaped zeroth-order antenna.

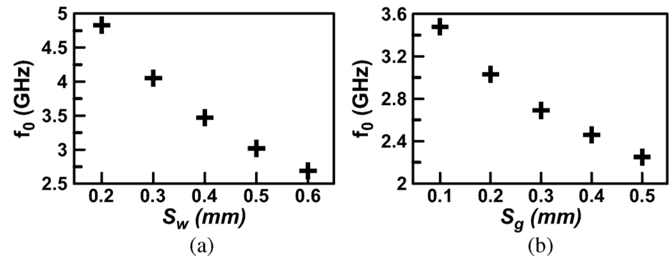

Fig. 3. Dependence of the zeroth-order resonant frequency on (a) the spiral width S_{W} with 1.25 winding turns and $S_{\mathrm{g}} = 0.2$ mm, and (b) the arm spacing S_{g} with 1.25 winding turns and $S_{\mathrm{W}} = 0.5$ mm.

inductance L_{L} need to be artificially created, whereas the series inductance L_{R} and shunt capacitance C_{R} result from the parasitic effect, contributing to the right-handed (RH) characteristic. When a CRLH transmission line is composed of N unit cells and is open-circuited, the CRLH resonator is formed and resonates at frequencies that satisfy

$$\beta_n = \frac{n\pi}{Np}, \qquad n = 0, \pm 1, \pm 2, \ldots\ldots, \pm(N-1) \tag{1}$$

where β_n corresponds to the propagation constant of the nth resonance mode and p is the physical length of the unit cell. When $n = 0$, the resonator operates at ZOR and becomes the zeroth-order resonator. In this mode, the structure supports infinite wavelength propagation, and its resonant frequency f_0 is solely determined by the lumped-element parameters as follows:

$$f_0 = \frac{1}{2\pi\sqrt{L_{\mathrm{L}} C_{\mathrm{R}}}}. \tag{2}$$

Since the resonant frequency is irrelevant to the physical length of the structure, the structure can be kept physically small while its resonant frequency is engineered to lower frequency by the lumped elements, indicating the potential for miniaturization.

The proposed CRLH unit cell is able to realize the series capacitance and shunt inductance in the single dual-arm spiral element. The geometry of the proposed dual-arm spiral-shaped zeroth-order antenna is depicted in Fig. 2. In each unit cell, the series capacitance C_{L} is developed by the edge coupling between the adjacent arms, and the shunt inductance L_{L} is resulted from the spiral arm shorted to the ground through the metallic via, as illustrated in Fig. 2. By increasing the number of winding turns, both of them can be easily increased, and the resonant frequency f_0 is decreased as a result. In practice, however, the increase in the number of spiral turns is limited by the rapidly decreased radiation efficiency, which will be discussed later. In order to excite the zeroth-order mode, in our structure, the via-hole is located at the arm that is not directly connected to the microstrip feed line. The proposed zeroth-order antenna consists of two unit cells and is fed by the microstrip line where a simple interdigital capacitor is used as the impedance matching network. In addition, the strip connected to the spiral in each unit cell is used to facilitate the impedance matching. In order to maintain low conductor loss, this strip was kept as short as possible while having relatively wide width. Thus, it mainly contributes to the shunt capacitance C_{R} and has a minor impact on the series inductance L_{R} in the equivalent circuit model.

For size reduction, the zeroth-order resonant frequency f_0 of the proposed dual-arm spiral-shaped antenna needs to be reduced as much as possible without considerably sacrificing its radiation characteristic. The spiral width S_{W} controls the effective coupling area between the signal and ground planes and thus determines the shunt capacitance C_{R} in the equivalent circuit model. On the other hand, the shunt inductance L_{L} can be enhanced by increasing the length of the spiral arm connected to the ground. Given the fixed number of spiral turns, this can be obtained by increasing the spacing between the adjacent arms S_{g}. Fig. 3 investigates the resonant frequency with respect to the spiral width S_{W} and the arm spacing S_{g}, respectively. As observed, the zeroth-order resonant frequency decreases as the spiral width or the arm spacing increases. In addition, the variation of the f_0 with respect to the number of the spiral turns is illustrated in Fig. 4(a). In spite of the fact that the resonant frequency f_0 can be effectively reduced and leads to further size reduction by increasing the number of spiral turns, the electrically smaller antenna combined with the increased conductor loss causes its radiation efficiency to drop significantly. It should be noted that in order to increase the prediction accuracy, the dielectric and the conductor losses were considered in the full-wave simulations. Similarly, the greater conductor loss associated with the decreased spiral width S_{w} or the increased ground width W_{g} degrades the radiation efficiency as shown in Fig. 4(b) and (c). Please note that in Fig. 4(b), the radiation efficiency decreases as S_{w} exceeds 0.4 mm. This can be explained as follows. While the conductor loss is decreased, the effective antenna aperture is reduced at lower resonant frequency, which dominates the radiation characteristic. Therefore, a compromise

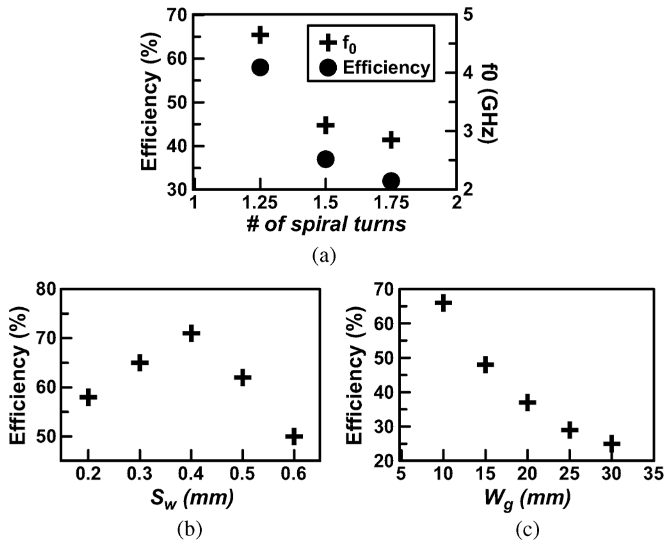

Fig. 4. Calculated radiation efficiency of the proposed dual-arm spiral-shaped antenna with respect to the structural parameters. (a) Radiation efficiency versus the number of spiral turns in the case of $S_w = 0.2$ mm, $S_g = 0.3$ mm, $d = 1$ mm, $D = 0.3$ mm, and $W_g = 20$ mm. The corresponding resonant frequency is also indicated. (b) Radiation efficiency versus the spiral width S_W in the case of $S_g = 0.2$ mm, $d = 1$ mm, $D = 0.3$ mm, $W_g = 20$ mm, and 1.25 winding turns. (c) Radiation efficiency versus the ground width W_g in the case of $S_w = 0.6$ mm, $S_g = 0.2$ mm, $d = 0.3$ mm, $D = 0.3$ mm, and 1.25 winding turns.

is needed in order to improve the overall antenna performance in terms of the compactness and radiation efficiency.

The radiation patterns of the zeroth-order resonant antenna depend on the particular feeding configuration employed. In the case when the coaxial line is used, the feeding line and the shorting via-holes are the main sources of radiation [6], [7], [12]. On the contrary, in the planar feeding configurations [8]–[10], the radiation mainly comes from the slots between the patches in the CRLH resonators where the main beam is in the broadside direction. In the present letter, the microstrip line is employed for fabrication convenience, and a simple interdigital capacitor is used as the matching network. Therefore, the radiation patterns are expected to be similar to the latter case, which will be confirmed in Section III.

III. Simulated and Experimental Results

In order to implement the zeroth-order resonant antenna operating at 2.45 GHz, the constitutive dual-arm spiral unit cell is properly designed so as to engineer the dispersion relation as desired. Fig. 5 shows the resulting dispersion curve where the zeroth-order resonance f_0 occurs at the transition frequency of the balanced unit cell and divides the dispersion diagram into the left-handed region and the right-handed region. It should be noted that this dispersion relation is derived on a basis of the dispersion characteristics of periodic structures and was calculated using the full-wave (HFSS) analysis of one unit cell.

The CRLH antenna based on two of the dual-arm spiral unit cells was simulated and fabricated. Referring to Fig. 2, the structural parameters of the proposed antenna are as follows: $S_w = 0.6$ mm, $S_g = 0.3$ mm, $D = 0.3$ mm, $i_w = 1.2$ mm, $i_g = 0.3$ mm, $d = 0.3$ mm, $x_p = 6.8$ mm, $g = 0.2$ mm, $e = 0.3$ mm,

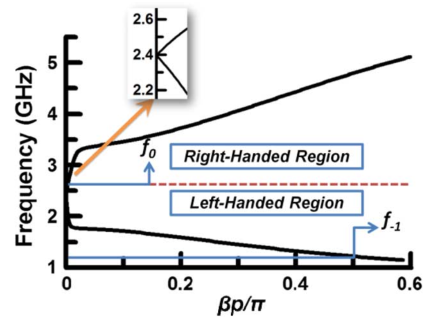

Fig. 5. Dispersion diagram of the proposed dual-arm spiral unit cell.

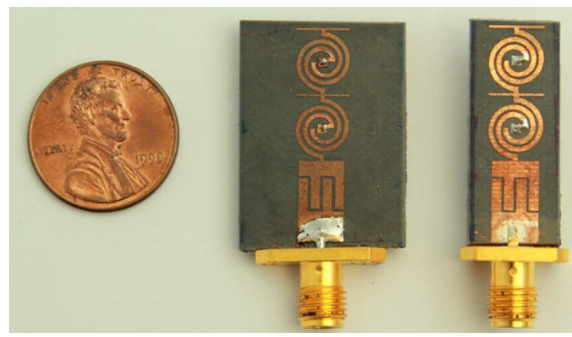

Fig. 6. Photograph of the fabricated antennas. The left and right antennas correspond to the cases of $W_g = 20$ mm and $W_g = 10$ mm, respectively.

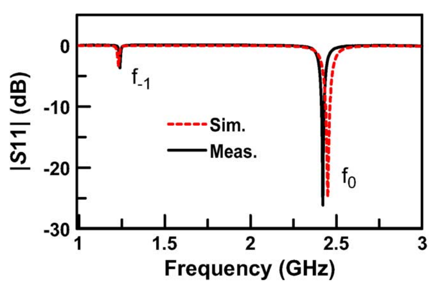

Fig. 7. Simulated and measured reflection coefficients of the proposed antenna with $W_g = 10$ mm.

$L_g = 26.4$ mm, and $W_g = 10$ mm. The photograph of the fabricated antennas is shown in Fig. 6. In order to confirm the dependence of the radiation efficiency on the ground width W_g, another antenna of identical physical parameters except with $W_g = 20$ mm (the left antenna) was also carried out. The proposed antennas were developed on the Rogers 5880 substrates of thickness 1.6 mm and dielectric constant 2.2.

The simulated and measured reflection coefficients of the antenna with $W_g = 10$ mm are illustrated in Fig. 7. Excellent agreement is obtained. The resonant frequencies at 2.42 and 1.23 GHz correspond to the zeroth-order resonance f_0 and negative first-order resonance f_{-1}, respectively. These resonances can be expected from the dispersion diagram shown in Fig. 5, where the two resonance modes are indicated. The observed resonant frequency shift may be attributed to the fabrication error and the deviation in the dielectric constant between the simulation and measurement. The measured 10-dB impedance bandwidth for the proposed antenna is about 1%.

Measurements of far-field radiation characteristics were taken in the anechoic chamber where the proposed antenna

TABLE I
SUMMARY OF ANTENNA PERFORMANCES FOR THE PROPOSED AND REFERENCE ANTENNAS

	This Work	[6]	[9]	[10]	[12]
Frequency (GHz)	2.42	2.3	2.03	2.97	2.44
Unit Cell Size (λ_0)	0.066 × 0.053 × 0.013	0.054 × 0.105 × 0.012	0.053 × 0.097 × 0.011	0.069 × 0.129 × 0.008	0.052 × 0.069 × 0.024
Antenna Footprint (λ_0)	0.218 × 0.082	0.23 × 0.146	0.172 × 0.145	0.218 × 0.218	0.325 × 0.325
Bandwidth (%)	1	1.3	6.8	1.8	1.44
Gain (dBi)	-0.53	-0.28	1.35	3.07	-6.83
Efficiecny (%)	53	62	62	75	15.21

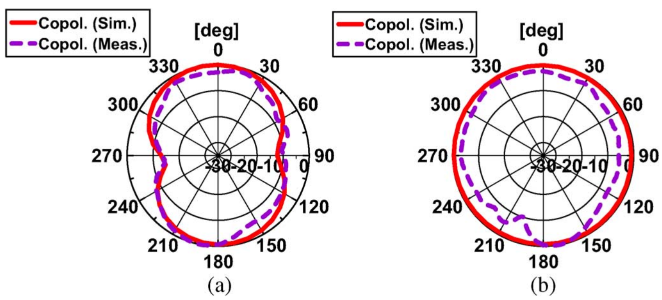

Fig. 8. Measured and simulated normalized radiation patterns of the proposed antenna with $W_g = 10$ mm. (a) E- plane (yz-plane). (b) H-plane (xz-plane).

receives signals from a standard horn antenna. The measured radiation patterns of the dual-arm spiral-shaped CRLH antenna with $W_g = 10$ mm are shown in Fig. 8. Experimental results agree well with the simulated data. The measured gain is -0.53 dBi that is close to the simulated gain of 0.02 dBi. In addition, the Wheeler cap method was applied to efficiency measurement. Compared to the simulated efficiency of 64%, the measured result is 53%, and this degraded efficiency is mainly attributed to two factors. First, as the measured gain is lower than the simulated one, the experimental efficiency is decreased as expected. Second, the imperfections in components and measurement setup may contribute to extra losses, such as the cable loss, connector loss, and imperfect electrical contact between the cap and ground plane. The dipolar radiation mode with the maximum radiation in the broadside direction and the omnidirectional radiation pattern in the H-plane are observed as expected. Combining with the operating frequency at 2.42 GHz, the proposed antenna lends itself to Bluetooth, RFID, or Wi-Fi applications [13]–[15]. Furthermore, compared to the antenna case of $W_g = 20$ mm where the measured gain is -1.75 dBi, this experimental result validates our previous investigation on the radiation capability with respect to the ground size. Table I summarizes the antenna performances of this work and the reference antennas in terms of electrical size, bandwidth, gain, and radiation efficiency. It can be shown that the proposed antenna is more compact while demonstrating comparable radiation capability.

IV. CONCLUSION

An alternative configuration for realizing the CRLH zeroth-order antenna is proposed and discussed in this letter. The dual-arm spiral unit cell is well suited to implement the four circuit elements in the CRLH resonators while occupying a small footprint. The proposed unit cell is only $0.066\lambda_0 \times 0.053\lambda_0$ at the operating frequency. Experimental and calculated results are provided and in good agreement.

REFERENCES

[1] T. K. Lo, C. O. Ho, Y. Hwang, E. K. W. Lam, and B. Lee, "Miniature aperture-coupled microstrip antenna of very high permittivity," *Electron. Lett.*, vol. 33, no. 1, pp. 9–10, Jan. 1997.

[2] B. Lee and F. J. Harackiewicz, "Miniature microstrip antenna with a partially filled high-permittivity substrate," *IEEE Trans. Antennas Propag.*, vol. 50, no. 8, pp. 1160–1162, Aug. 2002.

[3] P.-L. Chi, R. Waterhouse, and T. Itoh, "Antenna miniaturization using slow wave enhancement factor from loaded transmission line models," *IEEE Trans. Antennas Propag.*, vol. 59, no. 1, pp. 48–57, Jan. 2011.

[4] T. Fukusako, T. Terada, and K. Iwata, "Design and comparative study on planar small antennas using meander and peano line structure," in *Proc. IEEE AP-S Int. Symp.*, 2007, pp. 2451–2454.

[5] C. Caloz and T. Itoh, *Electromagnetic Metamaterials: Transmission Line Theory and Microwave Applications*. Hoboken, NJ: Wiley, 2006.

[6] S. Baek and S. Lim, "Miniaturised zeroth-order antenna on spiral slotted ground plane," *Electron. Lett.*, vol. 45, no. 20, pp. 1012–1013, Sep. 2009.

[7] S. Pyo, S. M. Han, J. W. Baik, and Y. S. Kim, "A slot-loaded composite right/left-handed transmission line for a zeroth-order resonant antenna with improved efficiency," *IEEE Trans. Microw. Theory Tech.*, vol. 57, no. 11, pp. 2775–2782, Nov. 2009.

[8] C.-J. Lee, K. M. K. H. Leong, and T. Itoh, "Composite right/left-handed transmission line based compact resonant antennas for RF module integration," *IEEE Trans. Antennas Propag.*, vol. 54, no. 8, pp. 2283–2291, Aug. 2006.

[9] T. Jang, J. Choi, and S. Lim, "Compact coplanar waveguide (CPW)-fed zeroth-order resonant antennas with extended bandwidth and high efficiency on vialess single layer," *IEEE Trans. Antennas Propag.*, vol. 59, no. 2, pp. 363–372, Feb. 2011.

[10] H. M. Lee and T. J. Cho, "Co-planar waveguide-fed zeroth-order resonant antenna with improved gain and efficiency," in *Proc. IEEE iWAT Int. Workshop*, 2011, pp. 388–391.

[11] W. Wang, X. Y. Cao, W. Y. Zhou, and T. Liu, "A novel compact uni-planar electromagnetic band-gap (UC-EBG) structure," in *Proc. ICMMT Int. Conf.*, 2008, pp. 1634–1636.

[12] Y. Dong, H. Toyao, and T. Itoh, "Miniaturized zeroth order resonance antenna over a reactive impedance surface," in *Proc. IEEE iWAT Int. Workshop*, 2011, pp. 58–61.

[13] J. Zhu, M. A. Antoniades, and G. V. Eleftheriades, "A compact tri-band monopole antenna with single-cell metamaterial loading," *IEEE Trans. Antennas Propag.*, vol. 58, no. 4, pp. 1031–1038, Apr. 2010.

[14] A. P. Saghati, M. Azarmanesh, and R. Zaker, "A novel switchable single- and multifrequency triple-slot antenna for 2.4-GHz Bluetooth, 3.5-GHz WiMax, and 5.8-GHz WLAN," *IEEE Antennas Wireless Propag. Lett.*, vol. 9, pp. 534–537, 2010.

[15] M.-T. Zhang, Y.-C. Jiao, and F.-S. Zhang, "Dual-band CPW-fed folded-slot monopole antenna for RFID application," *Electron. Lett.*, vol. 42, no. 21, pp. 1193–1194, Oct. 2006.